Synthesis and characterization of single-wall carbon nanotube–amorphous diamond thin-film composites

H. Schittenhelm, D. B. Geohegan,[a] and G. E. Jellison
Solid State Division, Oak Ridge National Laboratory, Oak Ridge, Tennessee 37831

A. A. Puretzky
Department of Materials Science and Engineering, University of Tennessee, Knoxville, Tennessee 37996

M. J. Lance
Metals and Ceramics Division, Oak Ridge National Laboratory, Oak Ridge, Tennessee 37831

P. F. Britt
Chemical Sciences Division, Oak Ridge National Laboratory, Oak Ridge, Tennessee 37831

(Received 6 June 2002; accepted for publication 17 July 2002)

Thin-film single-wall carbon nanotube (SWNT) composites synthesized by pulsed laser deposition (PLD) are reported. Ultrahard, transparent, pure-carbon, electrically insulating, amorphous diamond thin films were deposited by PLD as scratch-resistant, encapsulating matrices for disperse, electrically conductive mats of SWNT bundles. *In situ* resistance measurements of the mats during PLD, as well as *ex situ* Raman spectroscopy, current–voltage measurements, spectroscopic ellipsometry, and field-emission scanning electron microscopy, are used to understand the interaction between the SWNT and the highly energetic (~100 eV) carbon species responsible for the formation of the amorphous diamond thin film. The results indicate that a large fraction of SWNT within the bundles survive the energetic bombardment from the PLD plume, preserving the metallic behavior of the interconnected nanotube mat, although with higher resistance. Amorphous diamond film thicknesses of only 50 nm protect the SWNT against wear, providing scratch hardness up to 25 GPa in an optically transmissive, all-carbon thin-film composite. © *2002 American Institute of Physics.* [DOI: 10.1063/1.1506947]

Single-wall carbon nanotubes (SWNTs) exhibit exceptional mechanical,[1–3] electronic,[4] thermal, and optical properties[5] which are envisioned for new generations of strong, lightweight, multifunctional composites. SWNT are currently being explored in bulk polymer and metal–matrix composites with key difficulties encountered in dispersing the nanotubes and forming strong bonds to the matrix material.[6–8] In this report, pulsed laser deposition [(PLD), a versatile method for thin-film synthesis] is explored to encapsulate SWNT in a thin-film composite. Purified SWNT were sprayed from solution and dried to form disperse, electrically conductive interconnected mats on SiO_2 and Si substrates. Interconnected mats of SWNT exhibit pseudometallic behavior for a wide range of temperatures and applied fields,[9] and might be used to lend electrical conductivity, electrostatic protection, and thermal dissipation paths in matrices of polymers and other materials. In this study, a matrix of amorphous diamond [tetrahedrally coordinated amorphous carbon (ta-C)][10,11] was deposited by PLD to encapsulate the SWNT mats, forming a pure-carbon nanocomposite. The amorphous diamond film is intended to provide a hard, scratch-resistant, transparent, and electrically insulating coating for the electrically conductive, disperse mats of SWNTs and serve as an abrasion-resistant barrier to ambient gases and liquids, which have been observed to strongly influence the electronic properties of SWNT.[12,13]

The SWNTs were synthesized by laser vaporization[14] of a Dylon® target (with 1 at. % of Ni and Co each as catalysts) in a tube furnace at 1150 °C and 500 Torr argon (flowing at 200 sccm). The SWNT were purified from amorphous carbon and metallic catalyst particles by a procedure which involves etching for 16 h in 3 M HNO_3 in H_2O, followed by rinsing, drying, and subsequent oxidation for up to 90 min at ~500 °C.[15,16] Energy dispersive x-ray analysis and thermogravimetric analysis indicate that less than 0.5 wt. % of residual metal catalyst particles remain in the purified SWNT.

The purified SWNT were dispersed in distilled dichloroethane (DCE) at concentrations of about 1 μg/ml and spray deposited onto Si and SiO_2 (Suprasil fused silica) substrates with a commercial airbrush apparatus [see Fig. 1(a)]. The SWNT/DCE solution was sonicated during the spraying process to inhibit SWNT aggregation while a motorized $x-z$ stage was used to move the airbrush nozzle parallel to the substrate to obtain uniform SWNT dispersal on the substrates. By adjusting the spray duration, solvent concentra-

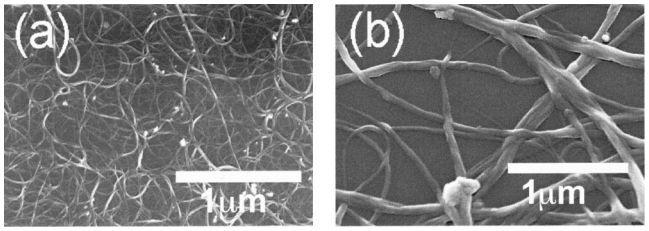

FIG. 1. Field-emission scanning electron microscopy images of (a) an uncoated SWNT mat on a Si substrate deposited by spray deposition of SWNT in dichloroethane, and (b) a SWNT/ta-C composite.

[a]Electronic mail: odg@ornl.gov

tion, nozzle pressure, and spraying strategy, the diameter of the bundles as well as the areal density of the interconnected SWNT mats could be controlled, thereby adjusting the resistance of the coating.

The nanotube laden substrates were then subjected to PLD conditions optimized for amorphous diamond film formation in a vacuum.[17] An ArF-excimer laser irradiated (energy density $F \sim 1.8\ \mathrm{J/cm^2}$) a pyrolytic graphite target in vacuum ($\sim 10^{-5}$ Torr), generating C^+ ions with most-probable kinetic energies ranging from 80–100 eV as measured with an ion probe.[18] These fast carbon ions and neutrals, along with slower C_2 and C_3 molecules, have sufficient kinetic energy to form amorphous diamond films on Si or SiO_2 substrates. However, it was unclear whether adherent films of amorphous diamond could be formed on webs of interconnected SWNT bundles which comprise up to 40% of the areal coverage (as shown in Fig. 1). After PLD in a vacuum (at $d=7$ cm), of film thicknesses between 10 and 50 nm [at rates of about 0.1 nm/s (0.01 nm/laser shot)], adherent films were found to conformally coat the SWNT in transparent, hard thin films as shown in Fig. 1(b).

An HP 4156A Precision Semiconductor Parameter Analyzer was first used to measure the current–voltage ($I-V$) characteristics of interconnected SWNT mats on SiO_2 substrates. Contact to the nanotube mat was made using evaporated Al pads on the SiO_2 which were deposited before nanotube spraying. All mats exhibited metallic behavior for applied voltages between -10 and $+10$ V, however depending upon the areal density of the nanotubes forming the mat, resistances were varied between 15 kΩ and 1 MΩ over 1 cm distances. A Keithley 195 System digital multimeter monitored the resistance of the SWNT mat *in situ* during deposition of the *ta*-C film, while the Al pads and contact leads were shielded from the PLD plume. In each case, an initial rapid increase in the resistance was observed after each of the first 5–10 PLD pulses which was probably caused by the desorption or damage of some of the SWNTs by the impact of the energetic carbon ions and neutrals. The resistance continued to increase slowly over the first few nm of film thickness, and then stabilize or decrease with further deposition. $I-V$ curves were then remeasured *ex situ*, and metallic behavior was again observed for the coated mats, however, the resistance ranged from a factor of 3 to a factor of 10^4 higher after *ta*-C film deposition (resistances from 45 kΩ to 10^4 MΩ). By comparison, resistances for pure *ta*-C films were 6×10^5 MΩ over a distance of 1 cm. In general, mats consisting of high areal densities and thicker bundles of SWNT resulted in smaller increases in resistance after deposition. In each case, the metallic behavior of the SWNT mat was preserved.

Spectroscopic ellipsometry measurements of a pure *ta*-C film and a representative *ta*-C/SWNT composite film (on a Si substrates) are shown in Fig. 2(a), which assumes a Tauc–Lorentz model with variable surface void fraction to account for surface roughness.[19] First, the pure *ta*-C film is of high quality, with a high ($n>2.5$) index of refraction and low absorption across the visible, corresponding to a band gap of 1.84 eV and a hardness of ~40 GPa.[18] The effective medium comprised of *ta*-C with embedded SWNTs exhibits a slightly lower refractive index and the expected higher absorptivity. However, good optical access to the embedded nanotubes is achieved since $k=0.19$ at 500 nm (close to 514 nm used for Raman probing) for the composite film, corresponding to an absorption coefficient of 48 000 $\mathrm{cm^{-1}}$ and an 80% transmission through the 50 nm thick film.

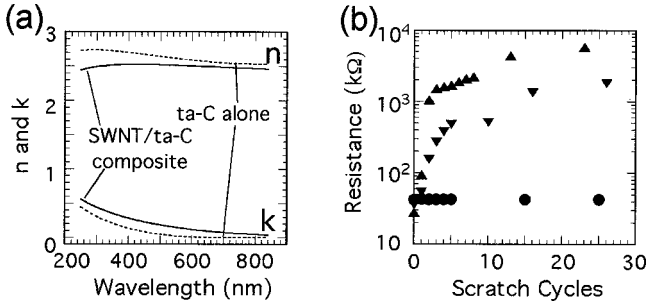

FIG. 2. (a) A comparison of the real (n) and imaginary (k) parts of the complex refractive index for a SWNT/*ta*-C composite film and a pure *ta*-C film (from spectroscopic ellipsometry). (b) Wear tests using a steel ball (15 GPa load) for two uncoated SWNT mats (triangles) and one *ta*-C-coated SWNT mat (circles) as measured by resistance of the mats over 1 cm distances.

Resonant Raman spectra from the SWNT mats before and after *ta*-C film deposition are shown in Fig. 3. Although decreased in magnitude, the characteristic tangential and breathing modes (TM and BM, respectively) are preserved indicating that a large fraction of SWNT survive the energetic deposition process. The Raman spectrum of the *ta*-C/SWNT composite in Fig. 3(b) displays a combination of the SWNT TM and a broad "*G*-band" from the amorphous diamond coating. Depending on the areal density of the SWNTs before *ta*-C film deposition the TM mode feature in the composite film ranges from barely observable to very pronounced [as in Fig. 3(b)]. A slight redshift of both the Raman BM and TM signals from the SWNTs was observed and is counterintuitive to the expected compressive strain of the SWNT from the *ta*-C film.

Figure 4 summarizes a model for *ta*-C/SWNT film formation consistent with the experimental results. High-energy C^+ ions and neutrals during PLD introduce defects in the upper layers of the SWNT bundles, affecting interconnections between bundles in the mats, resulting in the increased mat resistance. Kinetic model simulations with a Monte Carlo TRIM code estimated a ~1 nm penetration depth for 100 eV C^+ ions into SWNT bundles (estimated 1.33 $\mathrm{g/cm^3}$ density). Hence, defects should be located within a few upper layers of a SWNT bundle. After the first few nm of

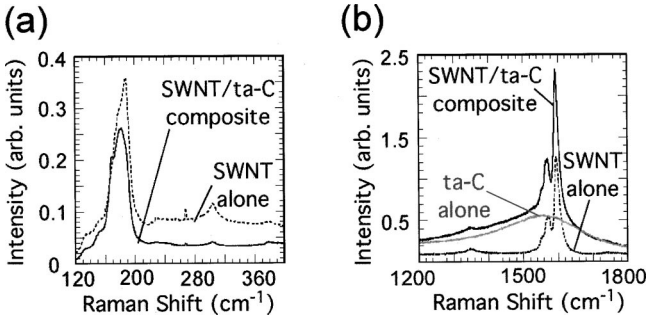

FIG. 3. Raman spectra of the SWNT mat using $\lambda=514$ nm excitation. (a) Radial BM with and without *ta*-C coating. (b) TM with and without *ta*-C coating, and Raman spectra of a pure *ta*-C film.

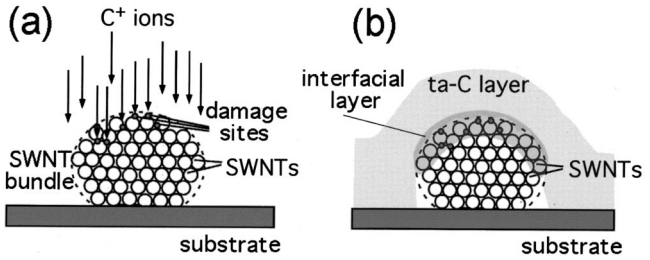

FIG. 4. Schematic of the proposed model for the formation of the SWNT–amorphous diamond thin-film composite using PLD. (a) Damaging of the SWNT bundle due to the impact of the fast carbon ions and neutrals. (b) Formation of an interfacial layer and build up of the *ta*-C coating.

amorphous diamond film formation, which requires the creation of an interfacial layer and reordering of the sp^2 bonds, the SWNT bundles should be protected from further damage. Thinner bundles thereby experience a higher defect ratio than thicker bundles. High areal densities, where parts of some bundles are shielded by others on top of them, lead to a lower ratio of damaged nanotubes.

The synthesized composites were tested for wear resistance and scratch hardness. A steel test ball (2 g load, approximately 1.2×10^{-3} mm^2 contact area, load $\sim$15 GPa) was moved across the SWNT mats on SiO_2 with and without protective amorphous diamond coatings while the resistance of the mats was monitored *in situ*. As shown in Fig. 2(b), the uncoated SWNT mats show a drastic increase in resistance after even one wear cycle. The resistance slowly saturates when the number of wear cycles exceeded 20. Scanning electron microscopy of the unprotected mat after wear testing showed that the thicker bundles were preferentially removed during the first few wear cycles, followed by the subsequent removal of thinner bundles. At the point of saturating resistance, only very thin bundles and single tubes were left on the surface to maintain conductivity of the mat. On the other hand, the *ta*-C/SWNT composite films showed high wear resistance compared to the uncoated mats. No increase in the resistance could be observed for up to 30 wear cycles. Scratch hardnesses of up to 25 GPa were measured for the *ta*-C/SWNT composite films on Si using a diamond scratch tester with a spherical diamond tip of 75 μm and loads between 10 and 100 g.

The results indicate that PLD can be used to form ultrahard, transparent, pure-carbon amorphous diamond thin films as matrices to encapsulate and provide scratch resistance for electrically conductive, disperse mats of SWNT. Moreover, PLD most often is performed in background gases where incident kinetic energies are far lower ($<$1 eV). PLD therefore appears to provide a versatile method to incorporate SWNT or nanowires into thin films for the exploration of multifunctional thin-film composites.

The authors gratefully acknowledge the assistance of P. H. Fleming, P. J. Blau, R. D. Ott, M. A. Guillorn, and T. E. Haynes. This work was supported in part by NASA Langley Research Center, and the Laboratory-Directed Research and Development Program at Oak Ridge National Laboratory, managed by UT-Battelle, LLC, for the U.S. Department of Energy under Contract No. DE-AC05-00OR22725.

[1] L. Vaccarini, C. Goze, L. Henrard, E. Hernandez, P. Bernier, and A. Rubio, Carbon **38**, 1681 (2000).
[2] R. S. Ruoff and D. C. Lorents, Carbon **33**, 925 (1995).
[3] Z. L. Wang, P. Poncharal, and W. A. de Heer, J. Phys. Chem. Solids **61**, 1025 (2000).
[4] T. W. Tombler, C. Zhou, L. Alexseyev, J. Kong, H. Dai, L. Liu, C. S. Jayanthi, M. Tang, and S. Y. Wu, Nature (London) **405**, 769 (2000).
[5] N. Minami, S. Kazaoui, R. Jacquemin, H. Yamawaki, K. Aoki, H. Kataure, and Y. Achiba, Synth. Met. **116**, 405 (2001).
[6] R. Andrews, D. Jacques, A. M. Rao, T. Rantell, F. Derbyshire, Y. Chen, J. Chen, and R. C. Haddon, Appl. Phys. Lett. **75**, 1329 (1999).
[7] R. Haggenmueller, H. H. Gommans, A. G. Rinzler, J. E. Fischer, and K. I. Winey, Chem. Phys. Lett. **330**, 219 (2000).
[8] C. Stephan, T. P. Nguyen, M. L. de la Chapelle, S. Lefrant, C. Journet, and P. Bernier, Synth. Met. **108**, 139 (2000).
[9] M. S. Fuhrer, W. Holmes, P. L. Richards, P. Delaney, S. G. Louie, and A. Zettl, Synth. Met. **103**, 2529 (1999).
[10] F. L. Xiong, Y. Y. Wang, V. Leppert, and R. P. H. Chang, J. Mater. Res. **8**, 2265 (1993).
[11] T. A. Friedmann, J. P. Sullivan, J. A. Knapp, D. R. Tallant, D. M. Follstaedt, D. L. Medlin, and P. B. Mirkarimi, Appl. Phys. Lett. **71**, 3820 (1999).
[12] A. Zahab, L. Spina, P. Poncharal, and C. Marliere, Phys. Rev. B **62**, 10000 (2000).
[13] S. Kazaoui, N. Minami, H. Kataura, and Y. Achiba, Synth. Met. **121**, 1201 (2001).
[14] A. A. Puretzky, D. B. Geohegan, X. Fan, and S. J. Pennycook, Appl. Phys. A: Mater. Sci. Process. **70**, 153 (2000).
[15] P. F. Britt, H. Schittenhelm, D. B. Geohegan, and A. A. Puretzky (unpublished).
[16] A. C. Dillon, T. Gennett, K. M. Jones, J. L. Alleman, P. A. Parilla, and M. J. Heben, Adv. Mater. **11**, 1354 (1999).
[17] A. A. Puretzky, D. B. Geohegan, G. E. Jellison, and M. M. McGibbon, Appl. Surf. Sci. **96**, 859 (1996).
[18] V. I. Merkulov, D. H. Lowndes, G. E. Jellison, A. A. Puretzky, and D. B. Geohegan, Appl. Phys. Lett. **73**, 2591 (1998).
[19] G. E. Jellison, Jr., V. I. Merkulov, A. A. Puretzky, D. B. Geohegan, G. Eres, D. H. Lowndes, and J. B. Caughman, Thin Solid Films **377**, 68 (2000).